

Methane in the Danube Delta: The importance of spatial patterns and diel cycles for atmospheric emission estimates

Anna Canning¹, Bernhard Wehrli^{2,3}, and Arne Körtzinger^{1,4}

¹GEOMAR Helmholtz-Zentrum für Ozeanforschung, Kiel, Schleswig-Holstein, Germany

²Institute of Biogeochemistry and Pollutant Dynamics, ETH Zürich, Zürich, 8092, Switzerland

³Eawag, Swiss Federal Institute of Aquatic Science and Technology, Kastanienbaum, 6047, Switzerland

⁴Christian-Albrechts-Universität zu Kiel, Kiel, Schleswig-Holstein, Germany

Correspondence: Anna Canning (acanning@geomar.de)

Abstract.

Methane (CH₄) is one of the substantial greenhouse gases in our atmosphere and its concentration has increased by ~ 4 % over the last decade. Although sources driving these increases are not well constrained, one potential contribution comes from wetlands, which are usually intertwined with rivers, channels and lakes, creating a considerable need to acquire higher resolution data to facilitate modelling and predictions. Here we took a fully contained sensor set-up to obtain measurements of CH₄, O₂ and auxiliary parameters, installed on a houseboat for accessibility, to assess and analyse surface water concentrations within the Danube Delta, Romania. During three expeditions in different seasons, we transected a ~ 400 km route with concentration mapping and two additional stations for monitoring diel cycles. Overall, the delta was a source for CH₄ throughout all seasons, with concentrations ranging between 0.113 – 15.6 μmol L⁻¹. Through calculated diffusive CH₄ fluxes for the overall delta, yielded an average of 49 ± 61 μmol m⁻² h⁻¹ corresponding to an extrapolated annual flux of 0.43 ± 0.53 mol m⁻² yr⁻¹. The dataset was split into three different subsystems; lakes, rivers and channels, with channels showing the highest variability. We found overlapping CH₄ concentrations throughout each subsystem, with large inflows coming from reed beds and channels into the lakes. Seasonal variability and water flow direction also influenced the overall dynamics in each region. We found large to extreme diel cycles in both the lakes and channels, with concentrations varying by an order of magnitude between these two systems. The lake diel cycle, showed a clear linear trend with an O₂:CH₄ molar ratio of -50:1 during the phase of nocturnal convection with the two water stratified bodies mixing during the night, suggesting daily vertical stratification allowing for macrophytes to create a temporal oxycline due to lack of light and movement between the stems as previously suggested, and potentially incurring an uncertainty range of a factor of 4.5. Our data illustrate the importance of high-resolution spatiotemporal data collection throughout the entire delta and the increased need for diel cycles in different habitats to improve the concentration and emission estimates from wetland systems.

1 Introduction

Methane (CH₄) is one of the most relevant anthropogenic greenhouse gases following carbon dioxide (CO₂) with an estimated global emission rate of 572 Tg CH₄ yr⁻¹ for the decade 2003-2012 (Saunois et al., 2020). More recently, we have seen an

accelerated increase from 1775 ppb in 2006 to 1850 ppb in 2017, and over a 100-year interval, CH₄ is 34 times more potent
25 as a greenhouse gas than CO₂ when including climate carbon feedbacks (28 times without feedbacks: Myhre et al., 2013; Schubert and Wehrli 2019). This continued increase has the potential to reverse any progress made for climate mitigation by reducing CO₂ emissions (Nisbet et al., 2019). Biogenic emissions from wetlands (Nisbet et al., 2019) contribute strongly to the overall estimate of 159 (117 – 212) Tg CH₄ yr⁻¹ from inland waters (Saunois et al., 2020). Although these emission numbers have high uncertainties, aquatic systems are known to act as net sources (Bastviken et al., 2011; Raymond et al., 2013). Inland
30 waters are known to have a significant CH₄ source strength and therefore, have seen an increase in attention (see Abril and Borges 2005; Panneer Selvam et al., 2014; Richey et al., 2002; Wang et al., 2009; Melton et al., 2013; Zhang et al., 2018).

Natural wetlands are one of the single largest sources of methane (125 – 218 Tg CH₄ yr⁻¹), accounting for roughly one third of total (anthropogenic and natural) emissions (Dean et al., 2018; Saunois et al., 2020). They are usual intertwined with rivers, channels and lakes making them highly diverse regions. Due to lakes being some of the easier systems to measure
35 and compare, they are the most extensively covered components of inland waters although only covering 0.9% of the Earth's surface. DelSontro et al. (2018) illustrate the large uncertainties in methane emission data. Depending on the upscaling methods these authors arrive at global CH₄ emission rates from lakes in the range of 78 – 248 Tg CH₄ C yr⁻¹. Specifically, shallow lakes are known to generally be hot spots in terms of CH₄ emissions (Cole et al., 2007; Davidson et al., 2018).

Rivers emit around 26.8 Tg CH₄ yr⁻¹ excluding ebullition (Stanley et al., 2016), however, due to a lack of global data
40 coverage and consistency their role in both carbon transport and storage is not well constrained (Tranvik et al., 2009). In general, there is a need for more detailed assessment of the role of rivers and channels for methane emissions as they have been suggested to be more spatiotemporally variable for CH₄ than CO₂ (Stanley et al., 2016; Natchimuthu et al., 2017).

Methane is produced in anaerobic environments, mostly within sediments (Schubert and Wehrli, 2019). Transport mechanisms to the atmosphere include turbulent diffusion through the water column followed by diffusive gas-exchange across the
45 water-air interface. Methane oxidizing bacteria in the water column reduces methane concentrations depending on the mixing regime. At high supersaturation and low hydrostatic pressure, bubbles can form and depending on their size ebullition offers a direct pathway from the sediments to the atmosphere (DelSontro et al., 2015).

With climate warming, CH₄ production is set to increase from lakes as well as through eutrophication (Marotta et al., 2014; Del Sontro et al., 2018, Sepulveda-Jauregui et al., 2018). Bartosiewicz et al., (2019) suggest that global warming will increase
50 surface water temperatures and strengthen lake stratification (Woolway et al., 2019). These authors suggest this may lead to an increase the CH₄ production in bottom waters potentially leading to +8% of the current global lake emissions from shallow (< 5 m) lakes. Therefore, analyzing the spatial and temporal (i.e. at least seasonal and diel) variability of methane emissions is important for future predictions and modelling efforts. Temporal variability, such as diel cycles of dissolved gases within inland waters, are driven by multiple processes including temporal variability of biological processes such as photosynthesis
55 and respiration, transportation, vertical stratification or temperature dependent solubility (Nimick et al., 2011; Maher et al., 2015; Zhang et al., 2018; Siczko et al., 2020). Although potentially substantial, these are rarely considered in studies of CH₄ fluxes due to general lack of data. Just as with overall data coverage of CH₄, both spatially and temporally, there is also need

for refined understanding of the contributions and the controls of CH₄ production and sources (Bogard et al., 2014; Abril and Borges 2019).

60 Given the complexity of inland water systems, especially wetland complexes, monitoring approaches were often focused on only one water type such as a river reach or a lake. Here we deployed an on-site monitoring device throughout the Danube delta, which measured gas concentrations continuously from a moving platform. The acquired high spatial and temporal resolution of methane concentrations and corresponding emissions formed a unique observational data basis. Continuous measurements across the delta allowed us to assess the importance of different systems (lakes, rivers and channels). The high-frequency data
65 at specific sites yielded insights into diel cycles and the specific day-night dynamics of methane emissions.

The Danube River Delta, as most river deltas, is known to be an important natural source of CH₄ (Cuna et al., 2008; Durisch-Kaiser et al., 2008; Pavel et al., 2009). Recently, Maier et al. (2021) investigated the seasonal emission rates of CO₂ and CH₄ in parts of the Danube Delta, focusing on a set of stations that were analyzed at monthly intervals. Here, we take a complementary approach with a measurement frequency up to 1 Hz. This allows not only for high-resolution data both in time and space but
70 also for a detailed look at the diel variability time-scale.

The objectives of this study are split into two main aspects: 1) to assess the differences between regions within the Danube delta in regards to CH₄ concentrations and fluxes, and 2) to use high-resolution data to explore the importance of a spatial variability and a diel cycle on local and regional concentrations and emission rates.

2 Methods

75 2.1 Set up

A portable and versatile flow-through sensor set-up was placed on-board a small houseboat for continuous mapping throughout the Danube Delta. Campaigns took place over three seasons: May (17 – 26), Aug (3 – 12), and Oct (13 – 23) 2017. The set-up consisted of the HydroC[®] CH₄ FT (CH₄ partial pressure, pCH₄, -4H-JENA engineering GmbH, Jena), HydroFlash[®] O₂ (dissolved oxygen, O₂, -4H-JENA) and a SBE 45 thermosalinograph (Sea-Bird Electronics, Bellevue, USA) to measure
80 temperature and conductivity. All sensors ran simultaneously at a speed of up to 1 Hz on the same continuous water flow (submersible pump deployed over the side at a depth of approx. 40 cm). The HydroC[®] CH₄ FT uses tunable diode laser absorption spectroscopy (TDLAS) technology, while the HydroFlash[®] O₂ Optode sensor uses the principle of dynamic fluorescence quenching (Bittig et al., 2018). Further details on the setup, its calibration and validation can be found in Canning et al. (2021).

85 2.2 Study site

The Danube River Delta is located on the Black Sea coast of Ukraine and Romania (44°25' – 45°30'N and 28°45' – 29°46'E). Originating in Germany, the Danube River travels across 2,857 km, with a drainage basin of 817,000 km² (Panin 2003). The delta is a complex system of wetlands, lakes, rivers and channels, both manmade and natural, with the largest compact reedbed

zone in the world (Oosterberg et al., 2000; Panin 2003). The fluvio-marine delta system accounts for 51% of the total area (Pavel et al., 2009) in which it sees salt intrusions and through-flow from the Black Sea into the delta. Since the 1970s, the Danube Delta has been subject to eutrophication, with its peak during 1987 – 1988 (Cristofor et al., 1993; Galatchi and Tudor 2006; Enache et al., 2019). After a decrease of nutrient loads in the 1990's, due to socioeconomic changes in Eastern Europe, a slow decline of nutrient levels was observed (Rîșnoveanu et al., 2004; Pavel et al., 2009), however, more recent levels comparable to those in 1988 were reported (Tudor et al., 2016; Spiridon et al., 2018).

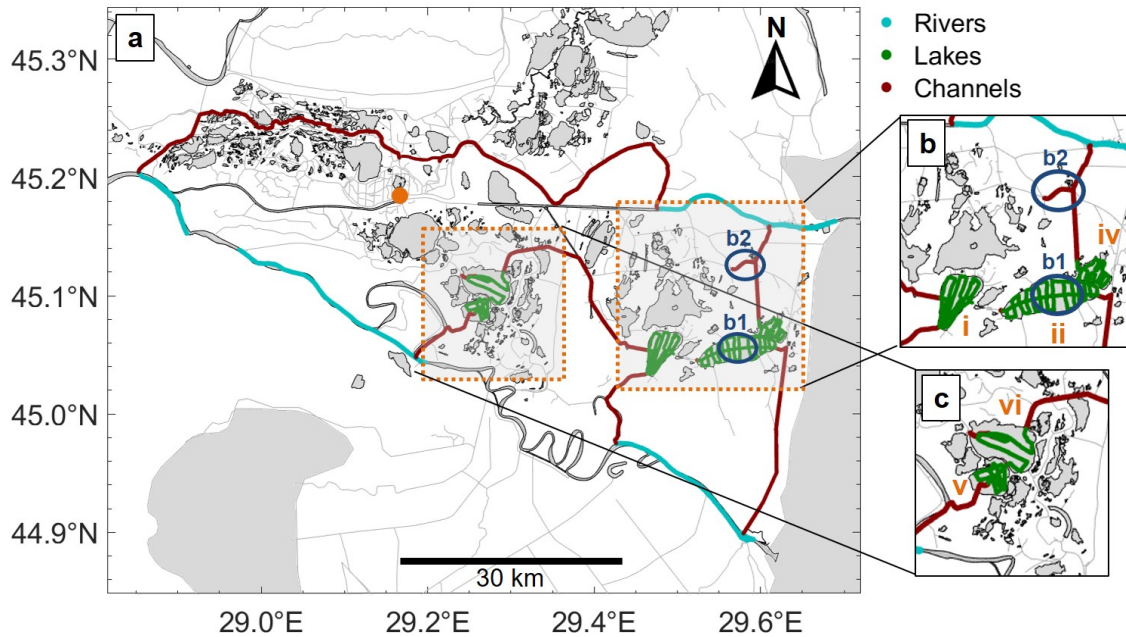


Figure 1. The Danube River Delta, Romania with the cruise tracks from the three seasonal campaigns split into rivers (blue), lakes (green) and channels (dark red). Systems of lake complexes in orange: Roșu-Puiu (b) and Gorgova-Uzlina (c). (b and c) show Lakes Puiu (b.i), Roșu (b.ii), Roșulete (b.iv), Uzlina (c.v) and Isac (c.vi). Blue circles indicate the sites of the two diel cycles at Lake Roșu (b1) and the ‘hot spot’ channel (b2), both during the August campaign. Gorgova meteo station located in the middle of the delta (orange dot). More in-depth labelling can be found in S1.3.

95 The delta is within the temperate climate system, but experiences broad annual ranges of air temperature from below freezing to more than 30°C (ICDP 2004). Deltas are continuously changing landscapes, with moving lake systems and floating islands. The overall Danube delta is roughly 4423 km² with a 67 – 81% coverage in either aquatic ecosystems (rivers, lakes and channels) or wetlands (Cristofor et al., 1993). In the anthropogenically modified Danube Delta we refer to the internal connections between the main river reaches and the lakes as channels (Kasprak et al., 2016). Using the small houseboat, the set-up was
 100 fixed, and a transect throughout the delta was carried out with extensive lake transects completed in all three seasons for comparability (Fig. 1), further details in Canning et al. (2021). The average total area covered was 380 km² across the entire delta

for each campaign, with an average measured distance of 107, 108 and 160 km² for rivers, lakes and channels respectively. Due to blockages in the channel between Lake Puiu and Lake Roşu, the transect had to be changed slightly between seasonal campaigns. This study also featured two stationary diel cycle measurements (Fig 1b: blue circles), one in Lake Roşu and the other in the channel where we observed a major biogeochemical ‘hot spot’ (S1.1).

2.3 Rivers, lakes and channels

Separation between rivers, lakes and channels was estimated visually where the boarder of the lake/channel/river starts and ends, ensuring the same regions were separated between the differing months. We classed channels as smaller bodies connecting between regions, with only the two larger branches as rivers, given their size, slightly faster flowing and greater depth. To statistically separate between rivers, lakes and channels a Kruskal-Wallis test was conducted due to the data being non-normally distributed (see S1.1 for visulisation of results). For CH₄, all regions were statistically different ($p < 0.001$). This was also the case between channels and the ‘hot spot’, which was assessed the same way ($p < 0.001$). Regions classed as between water boundaries, are areas such as channels leading into lakes; the mixing regimes between two systems. These occurred mainly in lakes where channels were entering and cross over of gas concentrations was observed (Fig. S4).

2.4 Computations of saturation and fluxes

The average global atmospheric CH₄ concentration (ppb) was taken from NOAA/ESRL Global Monitoring Division program (Dlugokencky 2019) for May, Aug and Oct 2017 (1847, 1844.7 and 1858.1 ppb respectively). These values were used due to negligible difference in the overall fluxes found when using other, more local values, due to the extreme water-side supersaturation. As the delta is practically sea level, barometric pressure as well as wind speed measured at the Gorgova station in the center of the delta were used (Fig. 1 orange dot). Schmidt numbers (Sc) were calculated for temperature dependence following (Wanninkhof 2014) for freshwater. The corrected Schmidt numbers varied between 296 and 824 in this study, consistent with the large temperature variance. Using CH₄ solubility (Wiesenburg and Guinasso 1979), CH₄ equilibrium concentrations in water were calculated and employed in the flux calculation. Fluxes were calculated following Peeters et al. (2019; supplementary material S3.2). Given slow stream velocities (with a maxima smaller than 30 cm s⁻¹, excluding flooding events), we used the parameterisation from Cole and Caraco (1998) with constant gas-transfer velocity of ~2 cm h⁻¹ in the absence of wind

$$k_{600} = 2.07 + 0.215 \cdot U^{1.7} \quad \text{cm} \quad \text{h}^{-1} \quad (1)$$

where U is wind speed at 10 m height in m s⁻¹, and k_{600} is the gas transfer velocity normalised to a Schmidt number of 600, i.e. CO₂ in freshwater at 20°C (Jähne et al., 1987; Crusius and Wanninkhof 2003):

$$k_{\text{CH}_4} = k_{600} \left(\frac{Sc_{\text{CH}_4}}{600} \right)^n \quad (2)$$

130 $for U \leq 3.7 m s^{-1} n = -\frac{2}{3}, for U > 3.7 m s^{-1} n = -\frac{1}{2}$

where k_{CH_4} is the transfer velocity at $S_{C_{CH_4}}$, which is the Schmidt number of CH_4 at a given temperature, and the exponential n reflects two wind speed regimes (Jähne et al., 1987). For rivers, due to differencing fetch and dynamics we used $n = -0.5$ throughout, consistent with multiple river studies (Borges et al., 2004; Guérin et al., 2007; Bange et al., 2019). The flux
135 was then calculated using the CH_4 concentration in the water and air:

$$\text{Flux} = k_{CH_4} \cdot (CH_{4,\text{water}} - CH_{4,\text{air}}) \quad \text{mol} \quad \text{m}^{-2} \quad \text{s}^{-1} \quad (3)$$

Given that the effect of spatial variability of k_{CH_4} is relatively small in lakes with surface areas of $5 \times 10^5 \text{ m}^2$ or larger (Schilder et al., 2013), we disregarded size effects of lakes on emission fluxes noted by Schilder et al. (2013). It is to be noted that these fluxes are estimates, and although wind was measured within the delta, the k_{600} value may vary significantly
140 from measured insitu wind values. Due to direct measurements collected previously in the years 2015 and 2016 (Maier et al., 2021), a comparison of k_{600} are shown in S1.2. In the following analyses, both day and night data will be shown unless stated otherwise for CH_4 .

3 Results and discussion

3.1 Concentrations distribution and estimated fluxes

145 Our high spatiotemporal resolution CH_4 data showed consistent supersaturation (CH_4 concentration range 0.113 to $15.6 \mu\text{mol L}^{-1}$), throughout the delta. Both a strong systemical and seasonal variability was observed, with channels having the highest concentrations of up to $15.6 \mu\text{mol L}^{-1}$ (Table 1) and showing overall a magnitude higher values compared to rivers. The concentrations are within the lower ranges previously observed (0.02 to $280 \mu\text{mol L}^{-1}$) for CH_4 in oxic freshwaters (Tang et al., 2016; Bižić-Ionescu et al., 2019).

150 Throughout the delta, high spatial variability was found across systems and water type boundaries (such as streams to lakes), which was also observed clearly by Crawford et al. (2017). More confined areas in closer proximity to the wetlands, were found to have the highest concentrations (further discussed below). These boundary crossovers, where higher concentrations were visible to proceeding regions, were due to seasonal changes in concentrations and change of flow direction varying throughout the delta (Fig. S4). This generally led to highly skewed CH_4 concentrations (Fig. 2), with generally rather low values, yet many
155 larger more dispersed values. In each season, 3 specific locations stood out with extreme CH_4 concentrations: the two channels joining Lake Puiu (Crisan channel: S1.3), and the ‘hot spot’ channel anomaly (Fig. 1b2, see S1.1 for visualisation of statistical significance $p < 0.001$). Rivers and channels (including the anomaly) showed the highest variability during Aug and May (Fig. 2), consistent with the directional flow regime bringing in the water from the surrounding wetlands after the flood waters. The highest median was observed during Oct for rivers, lakes and channels (median: 0.559 , 0.693 and $1.5 \mu\text{mol L}^{-1}$ respectively),
160 potentially due to macrophyte senescence and decomposition.

Oxygen (O_2) concentration in the water was mostly below saturation, however measurements were not distributed proportionally throughout the delta potentially leading to the lower median in May from more measurements collected in the ‘hot spot’. During Aug and Oct, O_2 saturation (%) was generally above 60% with Aug showing the largest variability above 100% coinciding with both temperature and production. However, O_2 saturation was frequently very low and undersaturated, indicating strong respiration in the water or flowing in from the reed belt. Wetland waters entering the fluvial systems are often de-oxygenated (Zuidgeest et al., 2016) and as the ‘hot spot’ stations represents sites receiving water from the wetland, it is likely not the only such site in the delta.

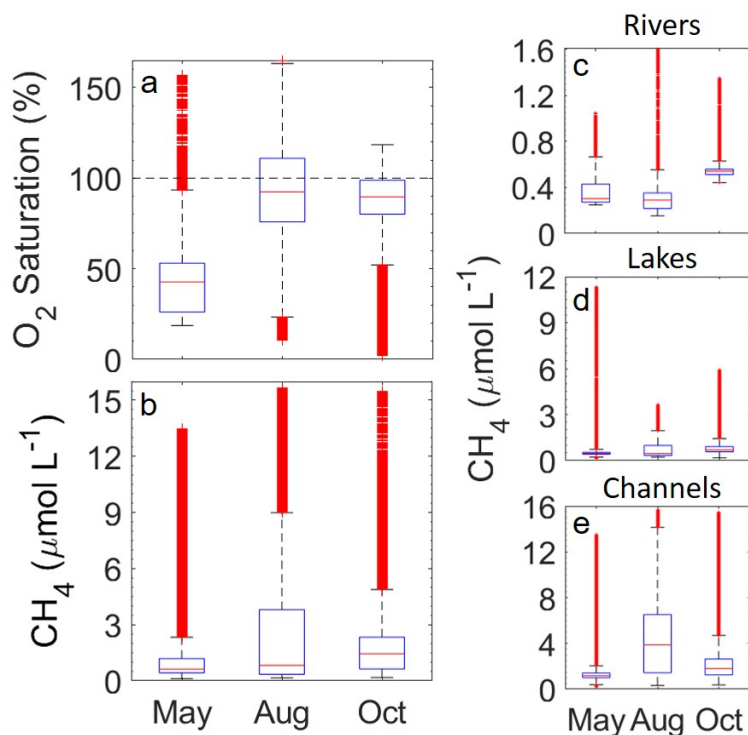


Figure 2. (a and b) Oxygen saturation (%) and CH_4 concentration ($\mu\text{mol L}^{-1}$) data from the three seasonal campaigns: May, August, and October. (c – e) CH_4 concentrations split by water type (rivers, channels and lakes). The blue boxes represent lower (25%) and upper (75%) quartiles, with the whiskers marking the lowest and highest data point within a distance of 1.5 times the interquartile range from the respective quartile. Red '+' signifies points outside of these boundaries. Median values are shown as horizontal red lines. All data are included ($n > 200,000$ for each season), including the hot spot and day/night cycle data.

Concentrations almost translate to the water-air fluxes (Fig. 3) which were calculated using wind data and therefore include the effect of wind speed. However, due to non-insitu measurements of the wind data, results should be seen as more of an estimate. We used the estimated area from Maier et al. (2021) for total area of rivers, channels and lakes (164, 33, 258 km^2 respectively) and the average emission rates in Table 1. By taking the average flux for each region across all seasons combined (Table 1), annual estimates for methane emissions of 16.1, 81.9 and 24.9 $\mu\text{mol m}^{-2} \text{h}^{-1}$, for rivers, channels and lakes,

175 respectively. The combined overall mean outgassing flux is then $49 \pm 61 \mu\text{mol m}^{-2} \text{h}^{-1}$. This gave an emission range of $2 - 5.4 \text{ t yr}^{-1} \text{ CH}_4$ for the combined region covered by rivers, lakes and streams (455 km^2). To give an estimate of the Danube on a global context, we used the mean estimated flux and applied this to the total area over the entire year. As the global overall average estimate for wetlands, lakes, streams and rivers of $117 - 212 \text{ Tg CH}_4 \text{ yr}^{-1}$ (Saunois et al., 2020), from a total area of $596 - 894$ million ha translates to an average global emission of $140 - 170 \mu\text{mol m}^{-2} \text{h}^{-1}$, this is about a factor of three higher than the flux rate obtained here for the Danube Delta. However, it is to be noted, our estimates are for diffuse fluxes were based on concentration measurements in the surface waters, therefore the influence by different processes are eliminated.

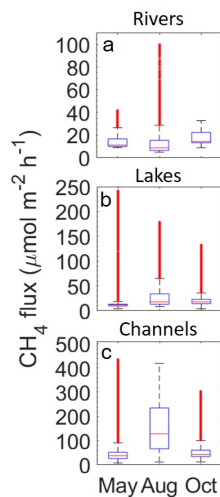


Figure 3. Calculated CH_4 fluxes ($\mu\text{mol m}^{-2} \text{h}^{-1}$) data from the three seasonal campaigns: May, August, and October for rivers (a), lakes (b) and channels (c). The blue boxes represent lower (25%) and upper (75%) quartiles, with the whiskers marking the lowest and highest data point within a distance of 1.5 times the interquartile range from the respective quartile. Red '+' signifies points outside of these boundaries. Median values are shown as horizontal red lines. All data are included ($n > 200,000$ for each season), including the hot spot and day/night cycle data.

180 In their study over two years, however, Maier et al. (2021) found evidence that bubble emission of methane in the Danube Delta lakes and channels, potentially accounted for $\sim 70 \%$. CH_4 fluxes calculated in this study were within the ranges of diffusive flux measurements reported by Maier et al. (2021) for rivers and lakes, whereas channels were within the range observed using their total fluxes (diffusive and potential ebullition fluxes), exceeding that of purely diffusive flux measurements. Median lake measurements within this study were about 63% lower than that reported by Maier et al. (2021), using total fluxes.

185 This coincides well with the $\sim 70 \%$ accountability for ebullition fluxes from lakes.

Although measured within the same regions, methods from both studies are not comparable due to the use of floating chambers at a few specific locations, potentially missing highly variable spatial variation and explaining the far larger diffusive fluxes found here in channels (Maier et al., 2021: $160 - 6200 \mu\text{mol m}^{-2} \text{d}^{-1}$, this study: $182 - 10500 \mu\text{mol m}^{-2} \text{d}^{-1}$). Further more, chamber measurements are focused on picking up ebullition fluxes, which can be high, whereas this study

190 estimates diffuse fluxes, based on concentration measurements in the surface waters. The two methods are therefore influenced by different processes, however, comparison of k_{600} can be found in S1.2.

Table 1. Range (minimum: Min, maximum: Max) and median (Med) of CH₄ concentrations ($\mu\text{mol L}^{-1}$), CH₄ saturation (%) and CH₄ flux ($\mu\text{mol m}^{-2} \text{h}^{-1}$) for rivers (R), channels (Ch) the 'hot spot' channel (HS) and lakes (L) over the 3 seasons: May, Aug and Oct 2017.

System		CH ₄			CH ₄ Saturation			CH ₄ Flux		
		$\mu\text{mol L}^{-1}$			%			$\mu\text{mol m}^{-2} \text{h}^{-1}$		
		May	Aug	Oct	May	Aug	Oct	May	Aug	Oct
R	Min	0.248	0.154	0.441	8560	6420	14200	8.9	4.9	8.8
	Med	0.302	0.290	0.541	10500	12200	17600	11.1	8.7	14.2
	Max	1.04	1.61	1.35	35600	66600	44600	42.1	101	33
Ch	Min	0.221	0.355	0.369	7990	14000	11800	7.6	11.6	11.9
	Med	1.17	1.30	2.23	40900	55700	71400	39	64.4	49.4
	Max	6.95	4.27	6.12	242000	180000	203000	225	220	165
HS	Min	1.03	1.83	0.994	34000	78600	32700	22.8	82.4	19.7
	Med	1.21	5.71	1.73	40400	237000	56900	32.1	212	36.1
	Max	13.5	15.6	15.5	469000	631000	507000	438	419	306
L	Min	0.113	0.224	0.177	4120	9450	5590	3.9	8.3	3.9
	Med	0.465	0.466	0.693	16100	19300	22300	11.8	17.7	17.8
	Max	11.3	3.65	5.93	395000	166000	187000	243	179	135

* Excluding the 'hot spot' and connecting channels, due to this location experiencing extremely high concentrations as an 'anomaly' within our full transect.

** Influence on edges from the channels into the lakes, across the border but meaning few meters of extreme concentrations.

3.1.1 Seasonality processes

195 Different processes influence the seasonal carbon turnover and methane production in the delta. High concentrations and therefore fluxes during May, have previously been explained due to growth, temperature and biomass peak, linking plant biomass to CH₄ emissions during growing season (Milberg et al., 2017). This can be further linked to the previous flood period just before the transect in May. Flooding will push oxygenated water into the reed stands and decrease emissions, while flood recession will move anoxic water from the reed into the channels and trigger ebullition (Gatland et al., 2014). Due to measuring following the flooding, this may potentially explain the elevated concentrations within the channel prior to the 'hot spot' (Fig.

200 4a red box). The Danube delta is known to have high levels of nutrients (Panin 2003; Durisch-Kaiser et al., 2008; Spiridon et al., 2018) arriving from the Danube river. This could account for CH₄ higher concentrations, and saturation due to enhanced plankton growth being a source of additional labile organic matter fuelling CH₄ productivity in the sediments, which then outfluxes (Mendonça et al., 2012; Ward et al., 2017).

Aug had the lowest water levels of each season, and although it showed the largest CH₄ range among the seasons, it had the 205 lowest measured median values, coinciding with the hypothesis that there is an overall decreased CH₄ concentration values during lower water levels (Melack et al., 2004; Marín-Muñiz et al., 2015; McGinnis et al., 2016). However, during Aug and Oct, the process of macrophyte degradation within the delta in both, lakes and channels, was linked with elevated CH₄ concentrations in specific locations (Fig. 4). This sharp increase of biodegradable organic matter could have been triggered anoxic decomposition of organic carbon which could have been responsible for released CH₄ (Segers 1998). This is visible in 210 Fig. 4d – f, although channels had higher CH₄ concentration, in Aug and Oct it is more visible of higher concentrations within the lakes (Fig. S4).

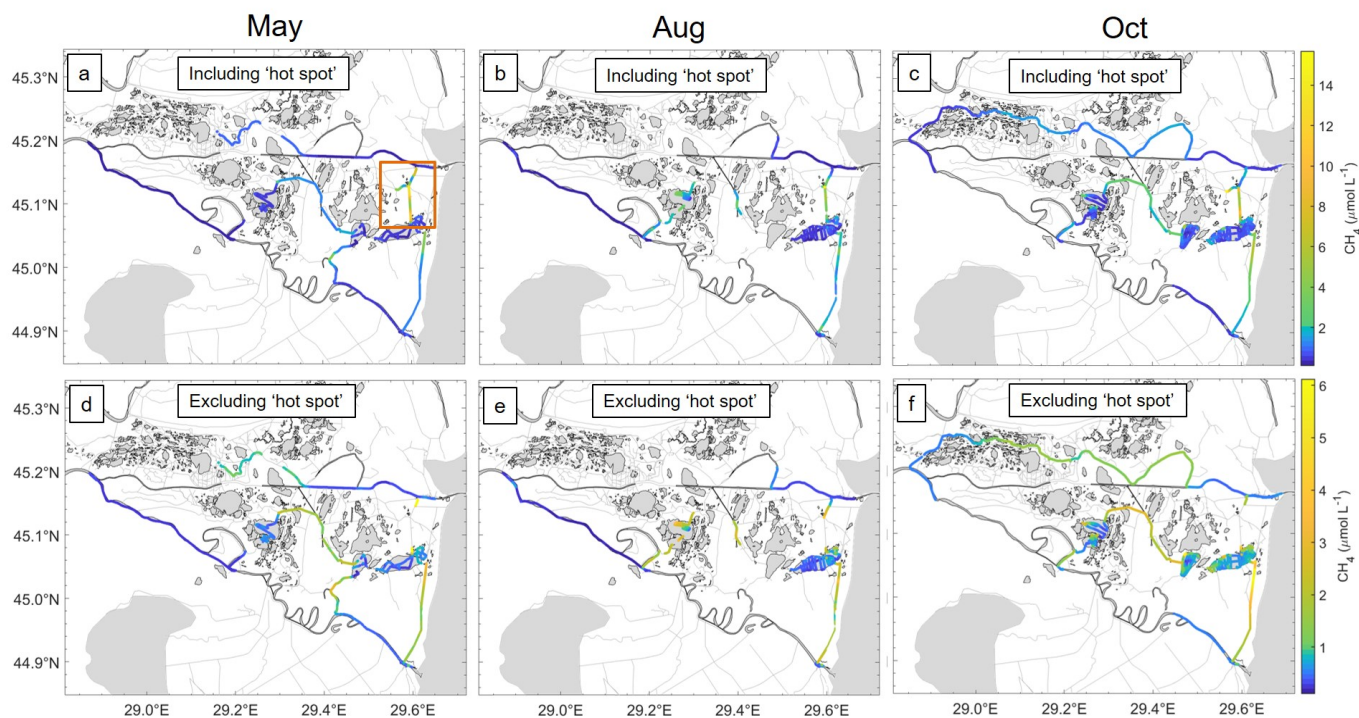


Figure 4. Spatial variability of CH₄ ($\mu\text{mol L}^{-1}$) over the 3 campaigns (May, Aug and Oct). Due to the 'hot spot' (Fig. 1b2) channel influencing the overall concentrations, (a – c) include the 'hot spot' measurements, reaching a maximum of $15.6 \mu\text{mol L}^{-1}$, (a red box) showing region of the 'hot spot'. (d – f) Spatial concentration of CH₄ ($\mu\text{mol L}^{-1}$) excluding the 'hot spot', with a maximum of $6.12 \mu\text{mol L}^{-1}$. Note the change and non-linear colouring of the colourbar for clearer overall CH₄ representation.

The channels are highly influenced by the surrounding reed beds, which are known to produce high levels of CH₄ (Bastviken et al., 2011), and have influence on the surrounding systems they flow into (e.g. lakes). This could explain the high variability (Fig. 2 and Fig. 4) and higher overall concentrations and fluxes (Table 1). They are also influenced from river reaches, channels and lakes that are sources of labile organic carbon fueling methanogenesis (Schubert and Wehrli 2019). However, given methanogenesis was not measured, we can only make assumptions about this.

Given delta systems are highly diverse, each region has been split to give a more descriptive assessment of the dynamics in the Danube delta.

3.1.2 'Hot Spot'

220 The 'hot spot' was classified as a small channel system receiving partially anoxic water from the reed stands (Fig. 1b (b1)). The highest conductivity was observed around the 'hot spot' as 0.08 S m⁻¹ (overall mean ± SD of 0.038 ± 0.005 S m⁻¹), suggesting also the potential of ground water influences (see Harvey et al., 1997). The 'hot spot' and adjacent channels were observed to be significantly different to other channels measured in this study ($p < 0.001$, S1.1).

225 Given the dramatic change within the concentrations and properties of the water, i.e. water temperature decreasing the further inwards we travelled, this would further provide evidence of influence from cooler groundwaters or potential waters from the reed beds also suggested by Maier et al. (2021). Groundwater can have an impact on overall gas supersaturation within the water column (Crawford et al., 2014a), potentially leading to increased CH₄ concentrations within specific locations throughout the delta. This was highly visible during Oct (Fig. 5c), where the highest concentrations were found closest to the end of the channel, where concentrations increased strongly. The channel leading to the 'hot spot' (Fig. 5), was adjacent to a large wetland with a more isolated lake within. The higher concentrations leading to the 'hot spot' are likely a consequence of waters from this large reed bed. This is emphasised during May (Fig. 5a), potentially via flood waters from the reed beds.

230

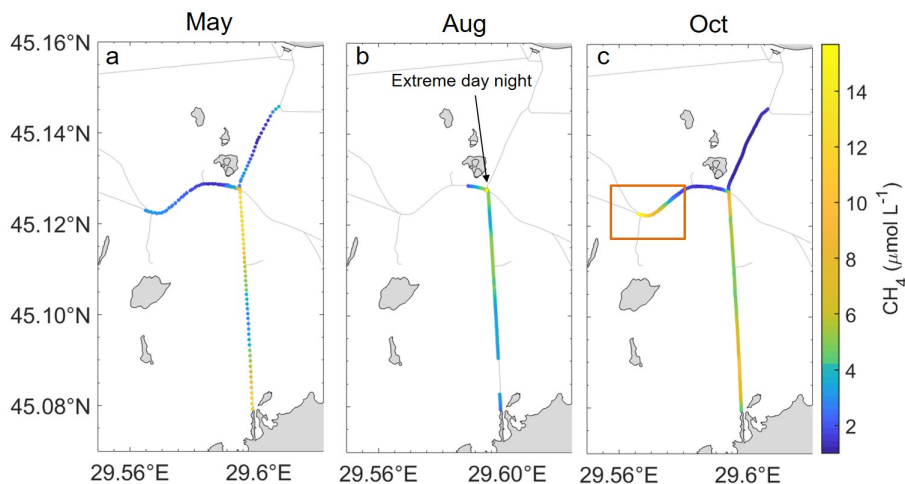


Figure 5. Spatial variability of CH_4 ($\mu\text{mol L}^{-1}$) over the 3 campaigns (May, Aug and Oct). Due to the 'hot spot' (Fig. 1b2) channel influencing the overall concentrations, figures a – c include this, reaching a maximum of 15.68 ($\mu\text{mol L}^{-1}$), (a red box) showing region of the 'hot spot'. (d – f) Spatial concentration of CH_4 ($\mu\text{mol L}^{-1}$) excluding the 'hot spot', with a maximum of 6.12 $\mu\text{mol L}^{-1}$. Note the change and non-linear colouring of the colourbar for clearer representation.

The 'hot spot' showed seasonality in concentrations and dynamics (Fig. 5). This can be seen clearly from the overall median values. Although the CH_4 median for both concentration and fluxes for May and Oct was similar to that of the channels, the ranges were almost doubled (Table 1). However, in Aug, fluxes measured a median of 212 ± 86.3 $\mu\text{mol m}^{-2} \text{h}^{-1}$ and had a concentration median four fold that of channels. However, combining all months together, the median from the 'hot spot' reduced to 54.9 ± 106 $\mu\text{mol m}^{-2} \text{h}^{-1}$. The influence of the 'hot spot' on the surrounding areas showed to have a strong influence, with high concentrations tending to disperse into the following channels (Canning et al., 2021). However, the influence of the 'hot spot' on the data as a whole system, is more dependant on the extension of this location. In the recent study by Maier et al. (2021), it was estimated that due to other similar environments within the delta, areas of little water movement, could account for 2% of the total channel area, or 20 % of CO_2 and CH_4 fluxes from the channels.

3.1.3 Fluvial CH_4

The fluvial delta (rivers and channels) works as the supply of incoming water into the main part of the delta, accounting for the base level of CH_4 concentrations being laterally transported. Based on continuous conductivity measurements, we found no evidence for saltwater intrusions from the Black Sea that could suppress methane production by high sulfate concentrations as suggested before (Durisch-Kaiser et al., 2008; Pavel et al., 2009). This would be important to explain reduced methane production as sulfate reduction becomes the dominating anaerobic mineralization pathway. Rivers had the lowest range of concentrations for CH_4 with the smallest variability out of all systems and the delta (Fig. 2 and Fig. 4). When excluding the 'hot spot', median values for channels were larger than those for rivers and fairly consistent throughout May and Aug, while increasing during Oct. While in comparison, the largest concentration was measured during May and Aug respectively, and

250 thereby changed the overall channel dynamics during Aug by increasing the overall channel median. The influence of the 'hot spot' showed what a strong influence one spot can have on a system, providing evidence that most of the CH₄ production happens within the delta, not the river itself.

As stated before, the estimated CH₄ fluxes followed roughly the same trend as CH₄ concentration, only moderately modulated by variable wind speed, therefore assessment of both will show a similar pattern. For rivers, such as with concentrations, Aug fluxes had the highest variability (Table 1 and Fig. 2) spanning from 4.9 to 101 $\mu\text{mol m}^{-2} \text{h}^{-1}$ CH₄, however had the lowest median of the seasons (8.7 $\mu\text{mol m}^{-2} \text{h}^{-1}$). Comparing fluxes from Oct to May and Aug fluxes for rivers, it had the largest percentile range and median (14.2 $\mu\text{mol m}^{-2} \text{h}^{-1}$). Channel fluxes from all months combined had a median of $47.9 \pm 70.6 \mu\text{mol m}^{-2} \text{h}^{-1}$, higher than both May and Aug alone (39.1 and 49.4 $\mu\text{mol m}^{-2} \text{d}^{-1}$: excluding the 'hot spot'). This was potentially linked to the increased degradation of macrophytes and other organic matter during Oct as stated before.

260 Overall our calculated mean flux for all months of the three campaigns from the fluvial delta was $594 \pm 525 \mu\text{mol m}^{-2} \text{h}^{-1}$, within the diffusive mean from the overall literature ($342.5 \pm 1062.5 \mu\text{mol m}^{-2} \text{h}^{-1}$; Sanley et al., 2016), yet with a far higher median of 473 $\mu\text{mol m}^{-2} \text{h}^{-1}$ (compared to 33.3 $\mu\text{mol m}^{-2} \text{h}^{-1}$). The fluvial delta had a mean of $2030 \pm 2.11 \mu\text{mol L}^{-1}$, with a median (1.52 $\mu\text{mol L}^{-1}$) comparable to that of Stanley et al. (2016) with a mean of $1.35 \pm 5.16 \mu\text{mol L}^{-1}$. When comparing within the fluvial system (rivers and channels separately), riverine CH₄ concentration during May and Aug had a median comparable to channels and therefore showed overall homogeneity, however channels appeared to have more extreme values and ranges than rivers. This difference would be due to less biological and physical processes occurring within the rivers due to depth, proximity to the wetlands and the flow generally being faster. However, both rivers and channels concentrations varied, showing large dependence on both seasonal changes and sample location.

From our meteorological data, we found little correlation with external factors such as wind, however, given these were not measured in situ, this cannot be fully quantified. We therefore suggest the observed distribution patterns over the entire delta are mostly more driven by both biological and physical processes affecting water-side CH₄ concentrations instead of effected by external factors, as previously suggested (Bange et al. 2019; Sanches et al. 2019) where precipitation was potentially responsible for a decrease in concentrations. Furthering evidence, just as with the 'hot spot', for strong spatiotemporal influence on CH₄ fluxes.

275 3.1.4 CH₄ dynamics in lakes

Lakes showed concentrations similar to those of Pavel et al. (2009) (see Table A1), although taken roughly 10 years later. The comparison to this earlier study indicates carbon turnover had not significantly changed during this period (Tudor et al., 2016; Spiridon et al., 2018). These concentrations ranged from the lowest 0.113 $\mu\text{mol L}^{-1}$ to the highest 11.3 $\mu\text{mol L}^{-1}$ both in May (largest concentration close to a channel). The median however, stayed roughly the same for both May and Aug (465 and 466 nmol L^{-1} respectively), with Oct reaching 0.63 $\mu\text{mol L}^{-1}$. We expect less productivity and more mineralization of macrophytes in Oct, leading to enhanced CH₄ production. Before entering each lake complex, the water had to travel through either the channels or the reed beds, increasing the concentrations coming into the lakes (shown clearly in Fig. S4). The inflowing water however quickly dispersed (Fig. 6), and was soon oxidized as seen before (Crawford et al., 2017). This inflow

was only visible on the edges of the lakes and although had influence on the overall concentration, were seen as outliers as the CH_4 appeared to potentially be quickly oxidized (Fig. 6). In Fig. 6, there is a clear visual dispersion of CH_4 from around the edges of the lake. This is specifically linked to an incoming channel and near by wetland with inflowing water. Directional water flow is also visible, with only certain regions of the lake experiencing higher concentrations (further examples in Fig. S4). Due to the mapping technique, heightened concentrations are shown to be visible in a moving direction: such as from one side of the lake to another, and not just a potential random CH_4 -high water parcel. The spatial differences and seasonal changes in the surface methane concentrations were far clearer in the lakes than the channels. Distribution of macrophytes in lakes could be linked to the map of O_2 and decaying plant biomass explained the high CH_4 levels in October (Milberg et al., 2017).

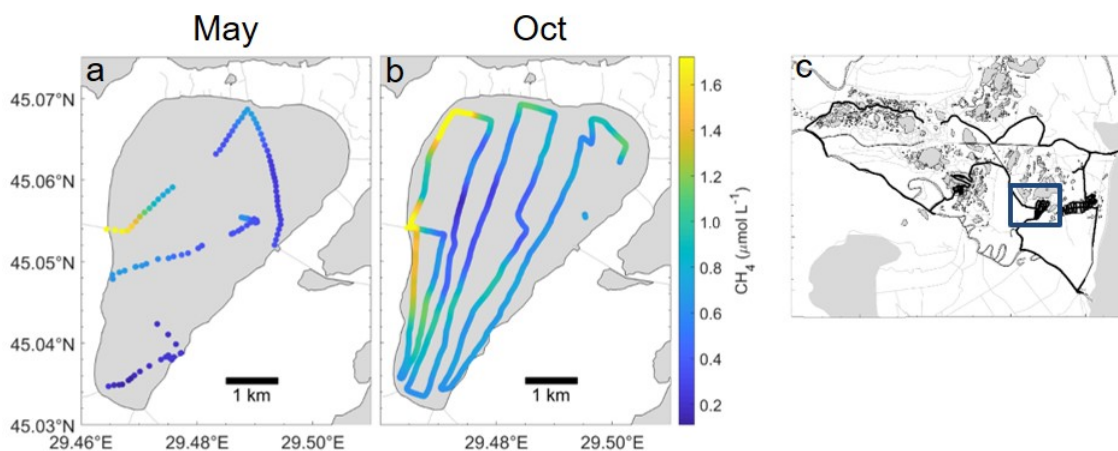


Figure 6. Spatial variability of CH_4 ($\mu\text{mol L}^{-1}$) over Lake Puiu during May (a) and Oct (b) from transect mapping completed over the course of a day. (c) Location of Lake Puiu within the transect throughout the Danube Delta. Channel influence can be observed closer to the edges of the lake from one direction, with concentrations reducing the closer to the middle of the lake.

By using the average fluxes of the measured lakes, we obtained the total lake area fluxes of 2.9, 6.5 and 4.8 mol CH_4 h^{-1} for May, Aug and Oct respectively. Diffusive release from sediments is usually the primary source of methane in surface waters (Peeters et al., 2019). Ebullition, however, adds a second pathway of CH_4 emissions to the atmosphere which is much more variable between systems and locations (see Bastviken et al., 2008, McGinnis et al., 2016, Schubert and Wehrli 2019 and van Bergen et al., 2019 for varying quantities). As it is not possible to capture ebullition through dissolved CH_4 surface measurements, such as in this study, this can potentially lead to mild-significant underestimations (Maier et al., 2021). However, the benefits of this study, were being able to pick up local dynamics that is usually missed by just daily or spot sampling.

3.2 Diel CH_4 cycling

One advantage to measuring continuously at high-resolution, was the opportunity to observe diel cycles. These extractions of temporal variability (i.e. over nearly a full 24 h cycle (Fig. 7)) were successfully carried out at specific locations. For analyses

and comparison, two diel cycles were recorded: one in Lake Roşu (Fig. 1b(ii)), and the other within the ‘hot spot’, both locations < 3 m depth. However it must be noted, that capturing the diel variability, few diel cycles were captured and these
305 may well be different at other times and locations and therefore not be representative of the overall situation in the delta.

Lake Roşu’s diel cycle (Fig. 7 a,c,e) showed clear indications of strong temporal variability on the diel time scale. The nocturnal buildup in CH₄ was linearly correlated with the loss of oxygen (molar CH₄:O₂ ratio 1:-50). CH₄ concentrations started from 0.4 μmol L⁻¹ at sunset and reached 1.4 μmol L⁻¹ at sunrise. During the diurnal period, CH₄ concentrations quickly relaxed back to initial conditions. As the mapping transect in Lake Roşu started around 9:00, some spatial variability
310 from varying concentrations due to proximity to the shore line (Fig. 8) is superimposed onto the dominant diel cycle, causing CH₄ concentrations to vary over the range 0.2 – 0.5 μmol L⁻¹. Overall, the CH₄ concentration showed a strong co-variation with oxygen. The diurnal relaxation of the CH₄ and O₂ concentrations to initial state had a more exponential shape. A possible explanation for this hysteresis: the water column stratified during the day, and underwent convective mixing as the surface water cooled during the night. This process progressively mixes the two formerly separated water bodies resulting in the observed
315 linear mixing line (Milberg et al., 2017). Diurnal warming then quickly re-stratified the water column so that the surface layer had no further entrainment from low-oxygen, high-methane waters below and underwent rapid CH₄ loss due gas exchange (Fig. 7). In contrast to oxygen, CH₄ did not reach equilibrium during the diurnal period. This could be due to continued supply from background sources of CH₄ (e.g. from macrophytes, lateral transport, diffusive flux across the thermocline or production via photoautotrophs (Bižić et al., 2020). Given the rate and extent of the CH₄ increase, this showed a potential CH₄ production
320 during the day in the bottom waters (Grasset et al., 2019), supporting the hypothesis of anoxic conditions close to the sediment and therefore intensified methanogenesis (Crawford et al., 2014b; 2017). This would be more likely to lead to other effective transport of CH₄ such as ebullition which could supply CH₄ to the surface waters or the atmosphere. Oxygen, in contrast relaxed back to equilibrium during the day as both air-water fluxes and in-situ photosynthetic production of O₂ would drive the system towards equilibrium. These concentrations, however, coincide with the mapping; higher CH₄ rates when closer to the
325 lake edges in Fig. 8), due to incoming waters from the wetlands.

During the day, Lake Roşu was supersaturated in O₂, indicating high levels of productivity in the surface waters, with O₂ moving away from equilibrium during the night. This is a potential indication for high rates of primary production during the day.

The ‘hot spot’ (Fig. 7b,d) also showed a clear co-variation of CH₄ with oxygen. Here CH₄ increases from roughly 4 to 16
330 μmol L⁻¹ over the nocturnal period (sunset to sunrise), followed by a rapid return to values around 6 μmol L⁻¹ during the diurnal period (sunrise to sunset). O₂ decreases while CH₄ stays roughly the same until around 3:30 am when it appeared to enter into hypoxic and even towards suboxic conditions as the ratio increased to about 1:3. This pronounced non-linearity is indicative of mixing with more than two endmembers, e.g., surface layer, sub-surface layer and a distinct bottom layer. The initial mixing encompassed only surface and sub-surface layer (similar to the lake situation) whereas later during the night,
335 near-bottom waters were entrained that have extremely elevated CH₄ concentration (and no oxygen) as a consequence of anoxic methanogenesis in sediment pore waters. An alternative explanation would be groundwater or lateral injection of water from adjacent wetlands.

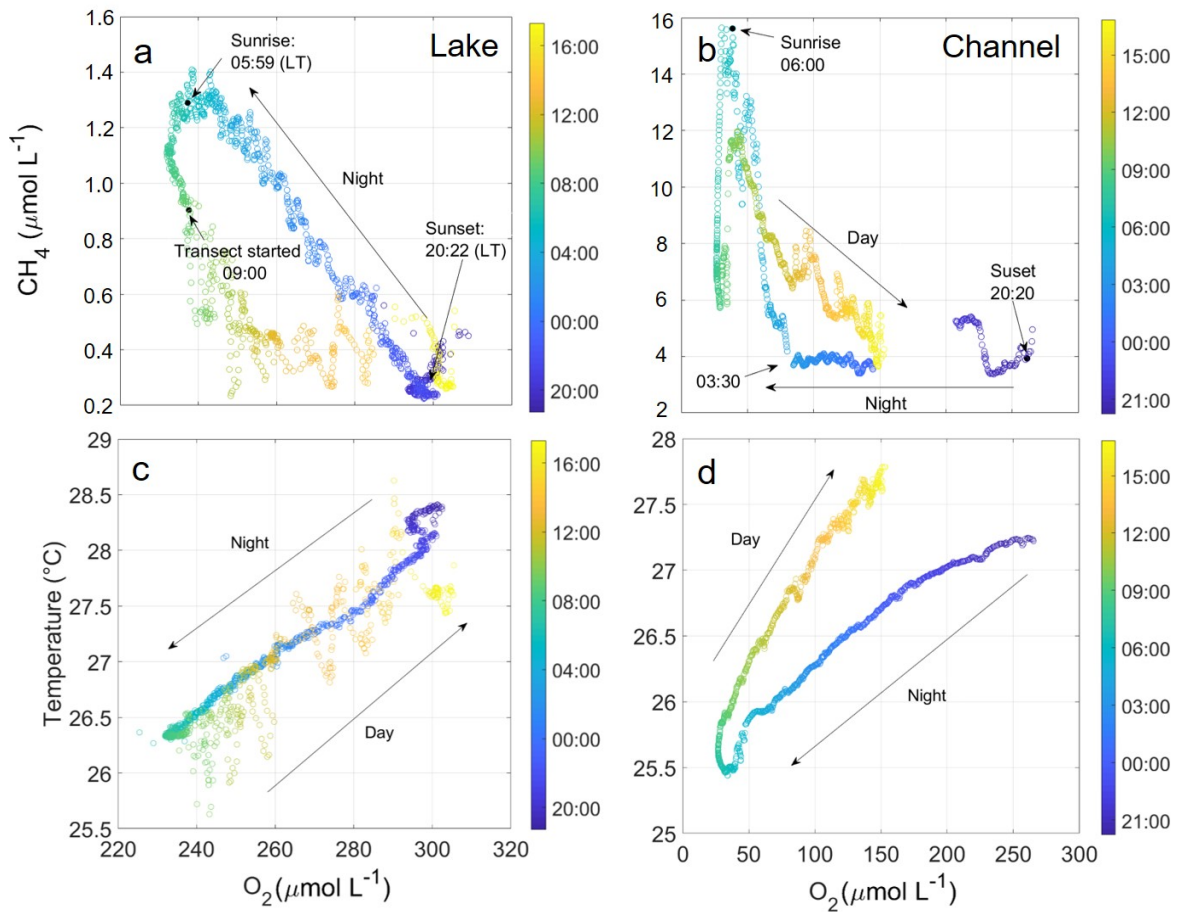


Figure 7. CH₄ (a + b) and temperature (c + d) against O₂ concentration as measured during diel cycle experiments in lake Rosu (left column) the 'hot spot' (right column). Colour bar denotes time of the day (hh:mm). Sunrise and sunset are also indicated. Both studies were carried out during the Aug (summer) campaign. During the night from just before 20:00 until 09:00, the boat was anchored and stationary. Transects through the following day continued to map the lake, whereas the channel was all in one anchored location.

The diel changes in temperature were roughly the same for the two situations ($\pm 2.5^{\circ}\text{C}$: Fig. 7), showing influence on all variables and induced strong density variations. The observed strong density variations were potentially sourced by the mixing of the bottom waters over the course of the night (Fig. 7), when cooling of the warm surface layer mixed with the colder bottom waters. It could be argued that temperature could have had an effect within the diel variability as previously suggested (Yvon-Durocher et al., 2014), although, temperature variability only causes a 3% change in methane solubility. Compared with the variability over the night, the transect during the day that covered the entire lake showed CH₄ generally staying consistent once the sun rose ($\sim 0.2 - 0.4 \mu\text{mol L}^{-1}$ with peaks due to shorelines), which was roughly the same concentration as the previous day, such as with all other variables. Statistically we also found no correlation between temperature and CH₄ flux (van Bergen

et al., 2019) over the entire lake ($p < 0.05$), therefore showing our diffusive fluxes are more reliant on the internal processes of the water.

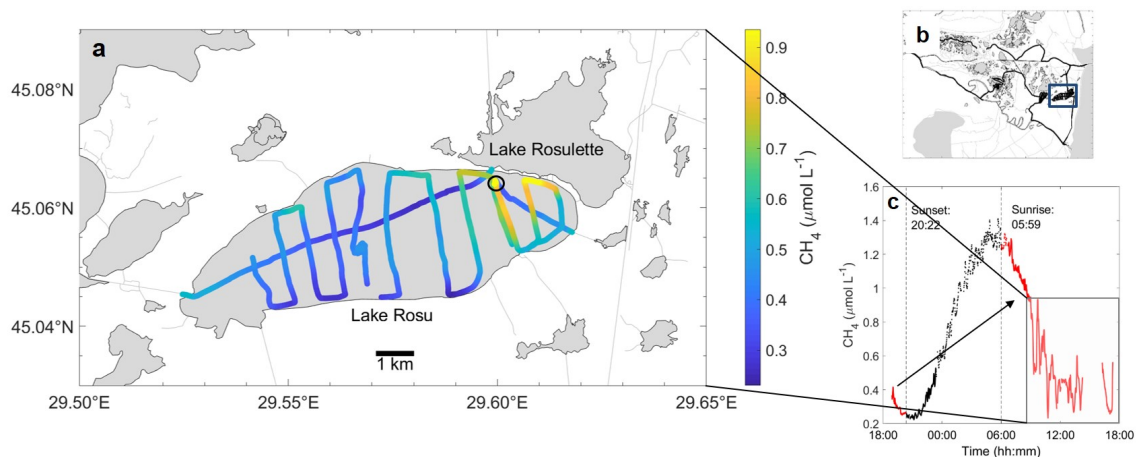


Figure 8. Mapping transect of lake Roşu (a), with the stationary location (a: circle), map the entire Danube delta with lake Roşu (b: blue square), and CH₄ concentration over time to show the distribution over the entire diel cycle (c: black showing between sunset and sunrise, red is day-time data, and box showing mapping transect). The data shown in c were used to calculate day light data (red) and the full daily cycle (all data in c). Location of diel cycle during the night shown in a: black circle .

To show the impact of these diel cycles, Fig. 9 summarizes the mean CH₄ concentrations and fluxes from the transect (~ 09:00 until 17:20, Fig. 8) and from the entire diel cycle (almost 24 hours: ~ 18:55 8th Aug 2017 until 17:20 9th Aug 2017).
 350 The mapping route is representative of a high spatial resolution mapping routine (Fig. 8). The diel cycle was observed within the mapping transect and therefore we were able to extract this section (Fig. 8c). Fluxes from the transect during the day (DL) and the full diel cycle (FD) were then scaled up to year averages showing an underestimation by just day light data alone. For the 'hot spot', we used the day night data (after sunrise) for this comparison due to no mapping transect following the diel cycle.

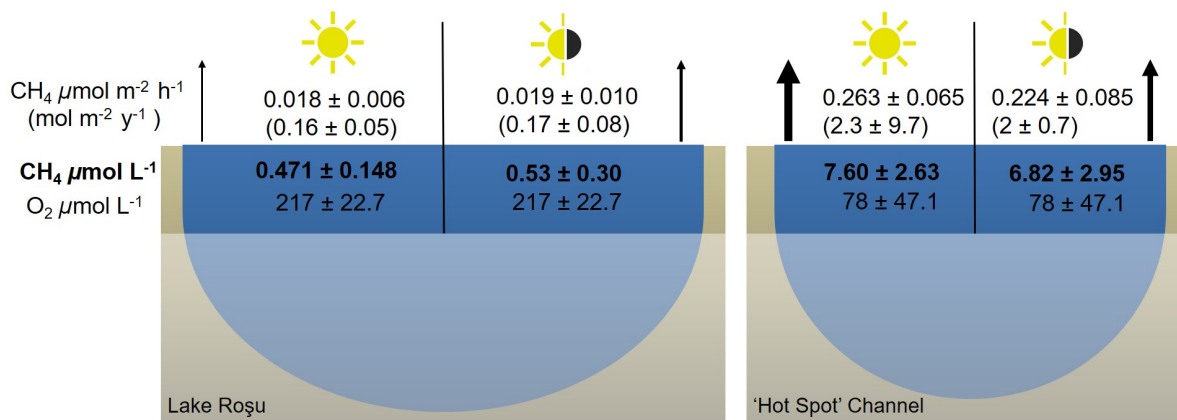


Figure 9. Mean methane fluxes on an hourly and annual basis as well as average concentrations of CH₄ and O₂ in Lake Roşu (left) and the "Hot spot" channel (right). Left half in each panel shows daylight data and right half present 24 hour coverage (Fig 8c). Thickness of arrows is a visual representation of flux scale: thicker the arrow the relatively larger flux compared to the other samples.

Overall, the values for day-light (DL) period and full day (FD) showed little difference due to the fact that the daily extremes are encountered around sunrise and sunset such that full coverage of the daylight hours captures the full dynamic range of the diel cycle (Fig. 9). Spot sampling without any knowledge of diel cycle variability therefore incurs an uncertainty range of a factor of 4.5 in this particular case, with the observed entire diel peak-to-peak amplitude approx. 0.3 – 1.3 μmol L⁻¹ in Lake Roşu and 2.5 – 14.5 μmol L⁻¹ in the hot spot channel.

Excluding all full diel cycles from the entire data set, the mean CH₄ flux decreased from 49 ± 61 μmol m⁻² h⁻¹ to 34.9 ± 35.7 μmol m⁻² h⁻¹, or a factor of 1.4. Therefore, scaling this by year changes the fluxes for the entire Danube delta from 0.4 ± 0.5 mol m⁻² h⁻¹ to 0.3 ± 0.3 mol m⁻² h⁻¹. Aug showed the largest variability when extracting diel cycles, with an uncertainty range of a factor of 2.27 from 84 ± 38 to 37 ± 33 μmol m⁻² h⁻¹. This greater variability can be linked to higher temperatures, greater stratification and increased production and organic matter degradation, all leading to potential increases in CH₄ (Duc et al., 2010; Fuchs et al., 2016). However, given diel cycles were not continuously measured throughout the entire system, these values merely illustrate the effect of neglecting or including diel cycle data. They do not represent ecosystem-wide fluxes because this analysis focuses only on diffusive fluxes and does not include the reed stands, with their own greenhouse gas dynamics.

There have been multiple studies looking into diel cycles (see Nimick et al., 2011; Zhang et al., 2018; van Bergen et al., 2019; Siczko et al., 2020 for examples), yet these are usually undetected or not fully resolved and therefore ignored, particularly in studies with sampling during daylight hours. This can lead to substantial under- or overestimation of emissions, as has also been noticed in systems with high CH₄ concentrations (Natchimuthu et al., 2017). Typically, delta systems tend to be either measured in specific regions (entrances or middle of lakes or channels), or with in situ measurements over time (e.g. Cuna et al., 2008; Wang et al., 2009; Olsson et al., 2015; Cunada et al., 2018). These measurements are then usually upscaled from single locations (e.g. Bouillon and Dehairs 2007; Borges et al., 2015; Joesoef et al., 2017), failing to include

375 spatial variability, system specific impacts (such as the ‘hot spot’ we observed here), and monthly changes. Here we can see that all of these impacts can have strong effects on the observed measurements.

4 Conclusions

To conclude, the overall Danube river delta surface waters were a source of CH₄, at a mean concentration of $1.7 \pm 1.93 \mu\text{mol L}^{-1}$ and calculated aquatic emission to the atmosphere of $0.43 \pm 0.53 \text{ mol m}^{-2} \text{ yr}^{-1}$. This is comparable to concentrations and diffusive flux mean of other systems of this type and size (see Stanley et al., 2016 for literature comparison: $1.35 \pm 5.16 \mu\text{mol L}^{-1}$ and $3 \pm 9.3 \text{ mol m}^{-2} \text{ yr}^{-1}$ and Maier et al., 2021). However, given that wetland systems (and therefore the reed beds) are known to be the significant in CH₄ fluxes of high variability (Segers 1998; Nisbet et al., 2019), our data only cover the water-air interface of channels, rivers and lakes and therefore may be underestimating the overall fluxes that include the vegetation cover of the wetlands. Being able to measure extensively within the lakes systems provided evidence that the reed bed concentrations were far higher than that of the lakes themselves. Our data have shown need for increased recordings of spatial observations on an intimate scale, along with diel cycles in all systems. Channels and lakes show far lower concentrations and fluxes when excluding diel cycles, while concentrations intertwine over the boarders. Of our three water types, rivers had the smallest concentrations and fluxes, showing that most of the CH₄ production must come from further within the wetlands. Most calculated CH₄ budgets, stem from extrapolations and data driven approaches due to lack of process-based models (Saunio et al., 2020), therefore investigations of the interactions between reed stands and open water will be of high priority. Strong influence from inflowing reed bed and channel water were also shown throughout this study throughout the three campaigns. From mapping transects, it was clear to see the dispersion of the CH₄ within the lake specifically, before oxidation would have occurred further into the lake.

With our analysis of diel cycles both in the channels and the lakes we were able to further confirm the importance high-resolution, spatiotemporal data collection. The diel cycle within the lake was consistent with the potential stratification over the day, where potentially vast amounts of organic carbon from macrophytes created anoxic subsurface waters, which slowly and steadily mixed during the night. Far larger quantities of CH₄ are released during the night due to daily stratification and a similar diel cycle was also active at the ‘hot spot’ site in a channel, where concentration changes varied four-fold between $4 - 16 \mu\text{mol L}^{-1}$ indicating that the process of advective cooling during the night, should also be considered in shallow systems.

In summary, spatial variability in and around lakes, reedbed edges and within channels should be one of the main areas of focus in terms of CH₄ release. On top of cross-boundary influences from high CH₄ regions, such as the reed beds, this is combined with comparing the overall peak-to-peak concentration ranges of observed diel cycles. We found there was a corresponding potential uncertainty of a factor of up to 4.5 within our measured lake (roughly 30%) due to diel variation. Using our measured examples with the diel cycles removed, accounted for a potential underestimation of up to 25% for channels, whereas an overestimation in lakes by 3.3% CH₄ concentration ($\mu\text{mol L}^{-1}$). Including our measured diel cycle measurements, accounted for roughly an increase of 20.4% in lakes and 4.2% decrease in channel fluxes. From this one study, this shows

compelling evidence the spatial variability should be considered more especially in delta regions, with more focus on lake edges and channels, while potential diel cycles should be accounted for.

Data availability. All data have been uploaded to PANGAEA, available at <https://doi.pangaea.de/10.1594/PANGAEA.925080>.

Table A1. Mean (\pm SD) for CH₄ concentration and flux ($\mu\text{mol L}^{-1}$ and $\mu\text{mol m}^{-2} \text{h}^{-1}$ respectively) and O₂ concentration ($\mu\text{mol L}^{-1}$) across all measured lakes during each expedition (May, Aug or Oct). Grey shows the comparison with Pavel et al. (2009) which was measured in 2006 as a comparison for CH₄ concentration and flux, in the same units for May and September.

Month	Lake Uzlina			Lake Isac			Lake Puiu			Lake Roşu			Lake Roşulete		
	May	Aug	Oct	May	Aug	Oct	May	Aug	Oct	May	Aug	Oct	May	Aug	Oct
2006	May	September	September	May	September	September	May	September	September	May	September	September	May	September	September
CH ₄ $\mu\text{mol L}^{-1}$	0.50 \pm	2.59 \pm	0.72 \pm	0.42 \pm	1.75 \pm	0.54 \pm	0.44 \pm	n.d.	0.80 \pm	468 \pm	0.53 \pm	0.76 \pm	0.97 \pm	0.82 \pm	
	0.08	0.39	0.29	0.06	0.83	0.23	0.30	0.30	0.64	0.08	0.30	0.30	1.59	0.43	0.52
Pavel et al. (2009)	0.71 \pm	0.64 \pm	0.22	0.57 \pm	0.61 \pm	0.16	0.89 \pm	n.d.		0.53 \pm	0.54 \pm	0.12	0.74 \pm	n.d.	
	0.26			0.37			0.42			0.11			0.58		
CH ₄ Flux $\mu\text{mol L}^{-1}$ $\text{m}^{-2} \text{h}^{-1}$	13 \pm	104 \pm	17 \pm	10.2 \pm	82.6 \pm	14.1 \pm	11.9 \pm	n.d.	17.8 \pm	11.8 \pm	19.3 \pm	21.6 \pm	21.7 \pm	31.6 \pm	29.3 \pm
	2.1	15.4	7.5	1.7	44.3	6	7.8		14.5	2.5	9.6	11.2	34.5	18.1	15.2
Pavel et al. (2009)	18 \pm	26 \pm	9	80 \pm	62 \pm	17	23 \pm	n.d.		13 \pm	7 \pm		11 \pm	n.d.	
	7			51			11			3			9		
O ₂ $\mu\text{mol L}^{-1}$	267	260	325	388	294	346	280	300	75.3	256	255	329	218	315	311
	\pm	\pm	\pm	\pm	\pm	\pm	\pm	\pm	\pm	\pm	\pm	\pm	\pm	\pm	\pm
	19	8	26.1	39	31.8	16.3	14.7	39.1	21.8	13.5	27.6	11.4	9.7	3.6	25

410 *Author contributions.* Anna Canning and Arne Körtzinger developed the concept and ideas of the study together. Anna Canning collected and processed the sensor data and wrote the manuscript. Arne Körtzinger and Bernhard Wehrli contributed ideas and clarifications of analyses. All authors reviewed and edited the manuscript.

Competing interests. All authors declare there is no conflict of interest.

415 *Acknowledgements.* The research leading to these results has received funding from the European Union's Horizon 2020 research and innovation program under the Marie Skłodowska-Curie grant agreement No 643052 (C-CASCADES project) and funding from Digital Earth which is coordinated by GEOMAR Helmholtz Centre for Ocean Research Kiel. We are grateful to Dennis Booge for assistance with the flux calculation. All of the -4H-JENA team with their support and help throughout my time with them and while on field work both day and night; all those who assisted on the cruises: our Romanian colleagues captain Nice, George, Marian, Christian Teodoru and Marie-Sophie Maier who drove the campaigns

420 **References**

- Abril, G., and Borges, A.V. (Eds): Carbon dioxide and methane emissions from estuaries. In Greenhouse gas emissions—fluxes and processes, 187–207. Springer, Berlin, Heidelberg, doi:10.1007/978-3-540-26643-3_8, 2005
- Abril, G., and Borges, A.V.: Carbon leaks from flooded land: do we need to re-plumb the inland water active pipe? *Biogeosciences*, 769–784, doi:10.5194/bg-2018-239, 2019
- 425 Bange, H. W., Sim, C.H., Bastian, D., Kallert, J., Kock, A., Mujahid, A., and Müller, M.: Nitrous oxide (N₂O) and methane (CH₄) in rivers and estuaries of northwestern Borneo, *Biogeosciences Discuss*, 1–5, doi:10.5194/bg-2019-222, 2019
- Bastviken, D., Cole, J.J., Pace, M.L., and Van de-Bogert, M.C.: Fates of methane from different lake habitats: Connecting whole-lake budgets and CH₄ emissions, *J. Geophys. Res. Biogeosciences*, 113, 1–13, doi:10.1029/2007JG000608, 2008
- Bastviken, D., Tranvik, L.J., Downing, J.A., Crill, P.M., and Enrich-Prast, A.: Freshwater methane emissions offset the
430 continental carbon sink, *Science* 331, 50, doi:10.1126/science.1196808, 2011
- Bartosiewicz, M., Przytulska, A., Lapierre, J. F., Laurion, I., Lehmann, M. F., and Maranger, R.: Hot tops, cold bottoms: Synergistic climate warming and shielding effects increase carbon burial in lakes, *Limnol. Oceanogr. Lett.*, 4, 132–144, <https://doi.org/10.1002/lol2.10117>, 2019.
- van Bergen, T.J.H.M., Barros, N., Mendonça, R., Aben, R.C., Althuisen, I.H., Huszar, V., Lamers, L.P., Lüriling, M., Roland,
435 F. and Kosten, S.: Seasonal and diel variation in greenhouse gas emissions from an urban pond and its major drivers, *Limnology and Oceanography*, 64, 2129–2139, doi:10.1002/lno.11173, 2019
- Bittig, H.C., Körtzinger, A., Neill, C., van Ooijen, E., Plant, J.N., Hahn, J., Johnson, K.S., Yang, B. and Emerson, S.R.: Oxygen Optode Sensors: Principle, Characterization, Calibration, and Application in the Ocean, *Front. Mar. Sci.*, 4, doi:10.3389/fmars.2017.0042018
- 440 Bižić-Ionescu, M., Ionescu, D., Günthel, M., Tang, K.W. and Grossart, H.P.: Oxidic Methane Cycling: New Evidence for Methane Formation in Oxidic Lake Water, *Biog. Hydrocarb.*, 379–400, doi:10.1007/978-3-319-78108-210, 2019
- Bižić, M., Klintzsch, T., Ionescu, D., Hindiyeh, M.Y., Günthel, M., Muro-Pastor, A.M., Eckert, W., Urich, T., Keppler, F. and Grossart, H.P.: Aquatic and terrestrial cyanobacteria produce methane, *Sci. Adv.*, 6, 1–10, doi:10.1126/sciadv.aax5343, 2020
- Bogard, M.J., Del Giorgio, P.A., Boutet, L., Chaves, M.C.G., Prairie, Y.T., Merante, A. and Derry, A.M.: Oxidic water column
445 methanogenesis as a major component of aquatic CH₄ fluxes, *Nat. Commun.*, 5, 1–9, doi:10.1038/ncomms6350, 2014
- Borges, A.V., Darchambeau, F., Teodoru, C.R., Marwick, T.R., Tamoo, F., Geeraert, N., Omengo, F.O., Guérin, F., Lambert, T., Morana, C. and Okuku, E.: Globally significant greenhouse-gas emissions from African inland waters, *Nat. Geosci.*, 8, 637–642, doi:10.1038/ngeo.2015.486, 2015
- Borges, A.V., Delille, B., Schiettecatte, L.S., Gazeau, F., Abril, G. and Frankignoulle, M.: Gas transfer velocities of CO₂ in
450 three European estuaries (Randers Fjord, Scheldt and Thames), *Limnol. Oceanogr.*, 49, 1630–1641, 2004
- Bouillon, S., Dehairs, F., Schiettecatte, L.S., and Borges, A.V.: Biogeochemistry of the Tana estuary and delta (northern Kenya), *Limnol. Oceanogr.*, 52, 46–59, 2007

- Canning, A., Körtzinger, A., Fietzek, P., and Rehder, G.: Technical note: Seamless gas measurements across Land-Ocean Aquatic Continuum – corrections and evaluation of sensor data for CO₂, CH₄ and O₂ from field deployments in contrasting environments, *Biogeosciences Discuss.*, doi:10.5194/bg-18-1351-2021, 2021
455
- Cole, J.J. and Caraco, N.F.: Atmospheric exchange of carbon dioxide in a low-wind oligotrophic lake measured by the addition of SF₆, *Limnol. Oceanogr.*, 43, 647–656, doi:10.4319/lo.1998.43.4.0647, 1998
- Cole, J.J., Prairie, Y.T., Caraco, N.F., McDowell, W.H., Tranvik, L.J., Striegl, R.G., Duarte, C.M., Kortelainen, P., Downing, J.A., Middelburg, J.J. and Melack, J.: Plumbing the Global Carbon Cycle: Integrating Inland Waters into the Terrestrial Carbon Budget, *Ecosystems*, 10, 172–185, doi:10.1007/s10021-006-9013-8, 2007
460
- Crawford, J.T., Loken, L.C., West, W.E., Crary, B., Spawn, S.A., Gubbins, N., Jones, S.E., Striegl, R.G. and Stanley, E.H.: Spatial heterogeneity of within-stream methane concentrations, *J. Geophys. Res. Biogeosciences*, 122, 1036–1048, doi:10.1002/2016JG003698, 2017
- Crawford, J.T., Lottig, N.R., Stanley, E.H., Walker, J.F., Hanson, P.C., Finlay, J.C. and Striegl, R.G.: CO₂ and CH₄ emissions from streams in a lake-rich landscape: Patterns, controls, and regional significance, *Global Biogeochem. Cycles*, 197–210, doi:10.1002/2013GB004661, 2014a
465
- Crawford, J.T., Stanley, E.H., Spawn, S.A., Finlay, J.C., Loken, L.C. and Striegl, R.G.: Ebullitive methane emissions from oxygenated wetland streams, *Glob. Chang. Biol.*, 20, 3408–3422, doi:10.1111/gcb.12614, 2014b
- Cristofor, S., Vadineanu, A., and Ignat, G.: Importance of flood zones for nitrogen and phosphorus dynamics in the Danube Delta, *Hydrobiologia*, 251, 143–148, doi:10.1007/BF00007174, 1993
470
- Crusius, J., and Wanninkhof, R.: Gas transfer velocities measured at low wind speed over a lake, *Limnol. Oceanogr.*, 48, 1010–1017, doi:10.4319/lo.2003.48.3.1010, 2003
- Cuna, S., Pendall, E., Miller, J.B., Tans, P.P., Dlugokencky, E., and White, J.W.: Separating contributions from natural and anthropogenic sources in atmospheric methane from the Black Sea region, Romania, *Appl. Geochemistry*, 23, 2871–2879, doi:10.1016/j.apgeochem.2008.04.019, 2008
475
- Cunada, C.L., Lesack, L.F.W., and Tank, S.E.: Seasonal Dynamics of Dissolved Methane in Lakes of the Mackenzie Delta and the Role of Carbon Substrate Quality, *J. Geophys. Res. Biogeosciences*, 123, 591–609, doi:10.1002/2017JG004047, 2018
- Davidson, T.A., Audet, J., Jeppesen, E., Landkildehus, F., Lauridsen, T.L., Søndergaard, M., and Syväranta, J.: Synergy between nutrients and warming enhances methane ebullition from experimental lakes, *Nat. Clim. Chang.*, 8, 156–160, doi:10.1038/s41558-017-0063-z, 2018
480
- Dean, J.F., Middelburg, J.J., Röckmann, T., Aerts, R., Blauw, L.G., Egger, M., Jetten, M.S., de Jong, A.E., Meisel, O.H., Rasigraf, O., and Slomp, C.P.: Methane Feedbacks to the Global Climate System in a Warmer World, *Rev. Geophys.*, 56, 207–250, doi:10.1002/2017RG000559, 2018
- DelSontro, T., del Giorgio, P.A., and Prairie, Y.T.: No Longer a Paradox: The Interaction Between Physical Transport and Biological Processes Explains the Spatial Distribution of Surface Water Methane Within and Across Lakes, *Ecosystems*, 21, 1073–1087, doi:10.1007/s10021-017-0205-1, 2018
485

- DelSontro, T., McGinnis, D. F., Wehrli, B., and Ostrovsky, I.: Size does matter: Importance of large bubbles and small-scale hot spots for methane transport, *Environ. Sci. Technol.*, 49, 1268–1276, <https://doi.org/10.1021/es5054286>, 2015.
- Dlugokencky, E, NOAA/ESRL: www.esrl.noaa.gov/gmd/ccgg/trendsCH4/, last access: 12 December 2019
- 490 Duc, N.T., Crill, P., and Bastviken, D.: Implications of temperature and sediment characteristics on methane formation and oxidation in lake sediments, *Biogeochemistry*, 100, 185–196, doi:10.1007/s10533-010-9415-8, 2010
- Durisch-Kaiser, E., Pavel, A., Doberer, A., Reutimann, J., Balan, S., Sobek, S., Radan, S. and Wehrli, B.: Nutrient retention, total N and P export, and greenhouse gas emission from the Danube Delta lakes, *Geo-Eco-Marina*, 81–90, doi:10.5281/zenodo.57332, 2008
- 495 Enache, I., Florescu, L.I., Moldoveanu, M., Moza, M.I., Parpală, L., Sandu, C., Turko, P., Rîșnoveanu, G. and Spaak, P.: Diversity and distribution of *Daphnia* across space and time in Danube Delta lakes explained by food quality and abundance, *Hydrobiologia*, 842, 39–54, doi:10.1007/s10750-019-04025-y, 2019
- Fuchs, A., Lyautey, E., Montuelle, B., and Casper, P.: Effects of increasing temperatures on methane concentrations and methanogenesis during experimental incubation of sediments from oligotrophic and mesotrophic lakes, *J. Geophys. Res. Bio-*
- 500 *geosciences*, 121, 1394–1406, doi:10.1002/2016JG003328, 2016
- Galatchi, L.D., and Tudor, M.: Europe as a source of pollution—the main factor for the eutrophication of the Danube Delta and Black Sea. In *Chemicals as Intentional and Accidental Global Environmental Threats*, 57-63, Springer, Dordrecht, 2006
- Gatland, J.R., Santos, I.R., Maher, D.T., Duncan, T.M., and Erler, D.V.: Carbon dioxide and methane emissions from an artificially drained coastal wetland during a flood: Implications for wetland global warming potential, *Journal of Geophysical*
- 505 *Research: Biogeosciences*, 119, 1698-1716, doi:10.1002/2013JG002544, 2014
- Grasset, C., Abril, G., Mendonça, R., Roland, F., and Sobek, S.: The transformation of macrophyte-derived organic matter to methane relates to plant water and nutrient contents, *Limnol. Oceanogr.*, 64, 1737–1749, doi:10.1002/lno.11148, 2019
- Guérin, F., Abril, G., Serça, D., Delon, C., Richard, S., Delmas, R., Tremblay, A., and Varfalvy, L.: Gas transfer velocities of CO₂ and CH₄ in a tropical reservoir and its river downstream, *J. Mar. Syst.*, 66, 161–172, doi:10.1016/j.jmarsys.2006.03.019,
- 510 2007
- Harvey, F. E., Lee, D. R., Rudolph, D. L., and Frape, S. K.: Locating groundwater discharge in large lakes using bottom sediment electrical conductivity mapping, *Water Resour. Res.*, 33, 11, 2609–2615, 1997.
- ICPDR international commission for the protection of the Danube river, 2004. The Danube River Basin District, Part A - Basin-wide over- view. WFD Roof Report
- 515 Jähne, B., Münnich, K.O., Bösinger, R., Dutzi, A., Huber, W., and Libner, P.: On the Parameters Influencing Air-Water Gas Exchange of magnitude lower in the water than in the air, information, which in turn has also hindered transfer in the water k₊, *J. Geophys. Res.*, 92, 1937–1949, doi:10.1029/JC092iC02p01937, 1987
- Joesoef, A., Kirchman, D.L., Sommerfield, C.K., and Wei-Jun, C.: Seasonal variability of the inorganic carbon system in a large coastal plain estuary, *Biogeosciences*, 14, 4949–4963, doi:10.5194/bg-14-4949-2017, 2017

- 520 Kasprak, A., Hough-Snee, N., Beechie, T., Bouwes, N., Brierley, G., Camp, R., Fryirs, K., Imaki, H., Jensen, M., O'Brien, G., Rosgen, D., and Wheaton, J.: The blurred line between form and process: a comparison of stream channel classification frameworks, *PLoS One*, 11, e0150293, doi:10.1371/journal.pone.0150293, 2016
- Maher, D.T., Cowley, K., Santos, I.R., Macklin, P. and Eyre, B.D.: Methane and carbon dioxide dynamics in a subtropical estuary over a diel cycle: Insights from automated in situ radioactive and stable isotope measurements, *Mar. Chem.*, 168, 69–79, 525 doi:10.1016/j.marchem.2014.10.017, 2015
- Maier, M.-S., Teodoru, C.R., and Wehrli, B.: Spatio-temporal variations in lateral and atmospheric carbon fluxes from the Danube Delta, *Biogeosciences Discuss.*, 1, 1417–1437, doi:10.5194/bg-18-1417-2021, 2021
- Marín-Muñiz, J.L., Hernández, M.E., and Moreno-Casasola, P.: Greenhouse gas emissions from coastal freshwater wetlands in Veracruz Mexico: Effect of plant community and seasonal dynamics, *Atmos. Environ.*, 107, 107–117, doi:10.1016/j.atmosenv.2015.02.03 530 2015
- Marotta, H., Pinho L., Bastviken D., Tranvik L. J., and Enrich-Prast A.: Greenhouse gas production in low-latitude lake sediments responds strongly to warming, *Nat. Clim. Change*, 4, 467–470. doi:10.1038/nclimate2222, 2014
- McGinnis, D.F., Bilsley, N., Schmidt, M., Fietzek, P., Bodmer, P., Premke, K., Lorke, A., and Flury, S.: Deconstructing Methane Emissions from a Small Northern European River: Hydrodynamics and Temperature as Key Drivers, *Environ. Sci. 535 Technol.*, 50, 11680–11687, doi:10.1021/acs.est.6b03268, 2016
- Melack, J.M., Hess, L.L., Gastil, M., Forsberg, B.R., Hamilton, S.K., Lima, I.B., and Novo, E.M.: Regionalization of methane emissions in the Amazon Basin with microwave remote sensing, *Glob. Chang. Biol.*, 530–544, doi:10.1111/j.1529-8817.2003.00763.x, 2004
- Melton, J.R., Wania, R., Hodson, E.L., Poulter, B., Ringeval, B., Spahni, R., Bohn, T., Avis, C.A., Beerling, D.J., Chen, G., 540 Eliseev, A.V., Denisov, S.N., Hopcroft, P.O., Lettenmaier, D.P., Riley, W.J., Singarayer, J.S., Subin, Z.M., Tian, H., Zürcher, S., Brovkin, V., van Bodegom, P. M., Kleinen, T., Yu, Z.C., and Kaplan, J.O.: Present state of global wetland extent and wetland methane modelling: conclusions from a model intercomparison project (WETCHIMP), *Biogeosciences*, 10, 753–788, doi:10.5194/bg-10-753-2013, 2013
- Mendonca, R., Kosten, S., Sobek, S., Barros, N., Cole, J.J., Tranvik, L., and Roland, F.: Hydroelectric carbon sequestration, 545 *Nat. Geosci.*, 5, 838–840, doi:10.1038/ngeo1653, 2012
- Milberg, P., Törnqvist, L., Westerberg, L.M., and Bastviken, D.: Temporal variations in methane emissions from emergent aquatic macrophytes in two boreonemoral lakes, *AoB Plants*, 9, doi:10.1093/aobpla/plx029, 2017
- Myhre, G., Shindell, D., Breion, F.M., Collins, W., Fuglestedt, J., Huang, J., Koch, D., Lamarque, J.F., Lee, D., Mendoza, B., Nakajima, T., Robock, A., Stephens, G., Takemura, T., and Zhang, H.: Anthropogenic and Natural Radiative Forcing. In: 550 *Climate Change 2013: The Physical Science Basis. Contribution of Working Group I to the Fifth Assessment Report of the Intergovernmental Panel on Climate Change* [Stocker, T. F., Qin, D., Plattner, G.-K., Tignor, M., Allen, S. K., Boschung, J., Nauels, A., Xia, Y., Bex, V., and Midgley, P. M., Cambridge Univ. Press. Cambridge, United Kingdom and New York, NY, USA, Chapter 8, 659–740, 2013

- Natchimuthu, S., Wallin, M.B., Klemetsson, L., and Bastviken, D.: Spatio-temporal patterns of stream methane and carbon dioxide emissions in a hemiboreal catchment in Southwest Sweden, *Sci. Rep.*, 7, 1–12, doi:10.1038/srep39729, 2017
- Nimick, D.A., Gammons, C.H., and Parker, S.R.: Diel biogeochemical processes and their effect on the aqueous chemistry of streams: A review, *Chem. Geol.*, 283, 3–17, doi:10.1016/j.chemgeo.2010.08.017, 2011
- Nisbet, E.G., Manning, M.R., Dlugokencky, E.J., Fisher, R.E., Lowry, D., Michel, S.E., Myhre, C.L., Platt, S.M., Allen, G., Bousquet, P., and Brownlow, R.: Very Strong Atmospheric Methane Growth in the 4 Years 2014–2017: Implications for the Paris Agreement, *Global Biogeochem. Cycles*, 33, 318–342, doi:10.1029/2018GB006009, 2019
- Olsson, L., Ye, S., Yu, X., Wei, M., Krauss, K.W., and Brix, H.: Factors influencing CO₂ and CH₄ emissions from coastal wetlands in the Liaohe Delta, Northeast China, *Biogeosciences*, 12, 4965–4977, doi:10.5194/bg-12-4965-2015, 2015
- Oosterberg, W., Buijse, A.D., Coops, H., Ibelings, B.W., Menting, G.A.M., Navodaru, I., and Török, L.: Ecological gradients in the Danube Delta lakes: present state and man-induced changes, *Lelystad Inst. Inl. Water Manag. Waste Water Treat. RIZA*, doi:90.369.5309x, 2000
- Panin, N.: The Danube Delta. Geomorphology and Holocene Evolution: a Synthesis / Le delta du Danube. Géomorphologie et évolution holocène: une synthèse, *Géomorphologie Reli. Process. Environ.*, 9, 247–262, doi:10.3406/morfo.2003.1188, 2003
- Panneer Selvam, B., Natchimuthu, S., Arunachalam, L., and Bastviken, D.: Methane and carbon dioxide emissions from inland waters in India - implications for large scale greenhouse gas balances, *Glob. Chang. Biol.*, 20, 3397–3407, doi:10.1111/gcb.12575, 2014
- Pavel, A., Durisch-kaiser, E., Balan, S., Radan, S., Sobek, S., and Wehrli, B.: Sources and emission of greenhouse gases in Danube Delta lakes, *Environ. Sci. Pollut. Res.*, 16, 86–91, doi:10.1007/s11356-009-0182-9, 2009
- Peeters, F., Fernandez, J.E. and Hofmann, H.: Sediment fluxes rather than oxic methanogenesis explain diffusive CH₄ emissions from lakes and reservoirs. *Sci. Rep.* 9: 1–10. doi:10.1038/s41598-018-36530-w, 2019
- Raymond, P.A., Hartmann, J., Lauerwald, R., Sobek, S., McDonald, C., Hoover, M., Butman, D., Striegl, R., Mayorga, E., Humborg, C. and Kortelainen, P.: Global carbon dioxide emissions from inland waters. *Nature* 503: 355–359. doi:10.1038/nature12760, 2013
- Richey, J.E., Melack, J.M., Aufdenkampe, A.K., Ballester, V.M., and Hess, L.L.: Outgassing from Amazonian rivers and wetlands as a large tropical source of atmospheric CO₂. *Nature* 416: 617–620. doi:10.1038/416617a, 2002
- Rîşnoveanu, G., Postolache, C., and Vădineanu, A.: Ecological significance of nitrogen cycling by tubificid communities in shallow eutrophic lakes of the Danube Delta, *Hydrobiologia*, 524, 193–202, doi:10.1023/B:HYDR.0000036133.92034.69, 2004
- Sanches, L.F., Guenet, B., Marinho, C.C., Barros, N., and de Assis Esteves, F.: Global regulation of methane emission from natural lakes, *Sci. Rep.*, 9, doi:10.1038/s41598-018-36519-5, 2019
- Saunois, M., Bousquet, P., Poulter, B., Peregón, A., Ciais, P., Canadell, J. G., Dlugokencky, E. J., Etiope, G., Bastviken, D., Houweling, S., Janssens-Maenhout, G., Tubiello, F. N., Castaldi, S., Jackson, R. B., Alexe, M., Arora, V. K., Beerling, D. J., Bergamaschi, P., Blake, D. R., Brailsford, G., Brovkin, V., Bruhwiler, L., Crevoisier, C., Crill, P., Covey, K., Curry, C., Frankenberg, C., Gedney, N., Höglund-Isaksson, L., Ishizawa, M., Ito, A., Joos, F., Kim, H.-S., Kleinen, T., Krummel,

- P., Lamarque, J.-F., Langenfelds, R., Locatelli, R., Machida, T., Maksyutov, S., McDonald, K. C., Marshall, J., Melton, J. R.,
590 Morino, I., Naik, V., O'Doherty, S., Parmentier, F.-J. W., Patra, P. K., Peng, C., Peng, S., Peters, G. P., Pison, I., Prigent, C.,
Prinn, R., Ramonet, M., Riley, W. J., Saito, M., Santini, M., Schroeder, R., Simpson, I. J., Spahni, R., Steele, P., Takizawa, A.,
Thornton, B. F., Tian, H., Tohjima, Y., Viovy, N., Voulgarakis, A., van Weele, M., van der Werf, G. R., Weiss, R., Wiedinmyer,
C., Wilton, D. J., Wiltshire, A., Worthy, D., Wunch, D., Xu, X., Yoshida, Y., Zhang, B., Zhang, Z., and Zhu, Q.: The global
methane budget 2000–2012, *Earth Syst. Sci. Data*, 8, 697–751, <https://doi.org/10.5194/essd-8-697-2016>, 2016.
- 595 Saunois, M., Stavert, A. R., Poulter, B., Bousquet, P., Canadell, J. G., Jackson, R. B., Raymond, P. A., Dlugokencky, E. J.,
Houweling, S., Patra, P. K., Ciais, P., Arora, V. K., Bastviken, D., Bergamaschi, P., Blake, D. R., Brailsford, G., Bruhwiler,
L., Carlson, K. M., Carrol, M., Castaldi, S., Chandra, N., Crevoisier, C., Crill, P. M., Covey, K., Curry, C. L., Etiope, G.,
Frankenberg, C., Gedney, N., Hegglin, M. I., Höglund-Isaksson, L., Hugelius, G., Ishizawa, M., Ito, A., Janssens-Maenhout,
G., Jensen, K. M., Joos, F., Kleinen, T., Krummel, P. B., Langenfelds, R. L., Laruelle, G. G., Liu, L., Machida, T., Maksyutov,
600 S., McDonald, K. C., McNorton, J., Miller, P. A., Melton, J. R., Morino, I., Müller, J., Murgia-Flores, F., Naik, V., Niwa, Y.,
Noce, S., O'Doherty, S., Parker, R. J., Peng, C., Peng, S., Peters, G. P., Prigent, C., Prinn, R., Ramonet, M., Regnier, P., Riley,
W. J., Rosentreter, J. A., Segers, A., Simpson, I. J., Shi, H., Smith, S. J., Steele, L. P., Thornton, B. F., Tian, H., Tohjima, Y.,
Tubiello, F. N., Tsuruta, A., Viovy, N., Voulgarakis, A., Weber, T. S., van Weele, M., van der Werf, G. R., Weiss, R. F., Worthy,
D., Wunch, D., Yin, Y., Yoshida, Y., Zhang, W., Zhang, Z., Zhao, Y., Zheng, B., Zhu, Q., Zhu, Q., and Zhuang, Q.: The Global
605 Methane Budget 2000–2017, *Earth Syst. Sci. Data Discuss.*, <https://doi.org/10.5194/essd-12-1561-2020>, 2020.
- Schilder, J., Bastviken, D., van Hardenbroek, M., Kankaala, P., Rinta, P., Stötter, T., and Heiri, O.: Spatial heterogeneity
and lake morphology affect diffusive greenhouse gas emission estimates of lakes, *Geophys. Res. Lett.*, 40, 5752–5756,
[doi:10.1002/2013GL057669](https://doi.org/10.1002/2013GL057669), 2013
- Schubert, C. J., and Wehrli, B.: Contribution of Methane Formation and Methane Oxidation to Methane Emission from
610 Freshwater Systems, in: *Biogenesis of Hydrocarbons*, Stams, A.J. M. and Sousa, D.. (Eds.), Springer International Publishing,
Chamber, 1–31, 2019
- Segers, R.: Methane production and methane consumption: A review of processes underlying wetland methane fluxes,
Biogeochemistry, 41, 23–51, [doi:10.1023/A:1005929032764](https://doi.org/10.1023/A:1005929032764), 1998
- Sepulveda-Jauregui, A., Hoyos-Santillan, J., Martinez-Cruz, K., Walter Anthony, K. M., Casper, P., Belmonte-Izquierdo, Y.,
615 and Thalasso, F.: Eutrophication exacerbates the impact of climate warming on lake methane emission, *Science of the Total
Environment*, 636, 411–419, [doi:10.1016/j.scitotenv.2018.04.283](https://doi.org/10.1016/j.scitotenv.2018.04.283), 2018
- Sieczko, A.K., Duc, N.T., Schenk, J., Pajala, G., Rudberg, D., Sawakuchi, H.O., and Bastviken, D.: Diel variability of
methane emissions from lakes, *Proceedings of the National Academy of Sciences*, 117, 21488–94, [doi:10.1073/pnas.2006024117](https://doi.org/10.1073/pnas.2006024117),
2020
- 620 Spiridon, C., Teodorof, L., Burada, A., Despina, C., Seceleanu-Odor, D., Tudor, I.M., Ibram, O., and Georgescu, L.P.:
Seasonal variations of nutrients concentration in aquatic ecosystems from Danube delta biosphere reserve, *AACL Bioflux*, 11,
1882–1891, 2018

- Stanley, E.H., Casson, N.J., Christel, S.T., Crawford, J.T., Loken, L.C., and Oliver, S.K.: The ecology of methane in streams and rivers: Patterns, controls, and global significance, *Ecol. Monogr.*, 86, 146–171, doi:10.1890/15-1027, 2016
- 625 Tang, K.W., McGinnis, D.F., Ionescu, D., and Grossart, H.P.: Methane production in oxic lake waters potentially increases aquatic methane flux to air, *Environ. Sci. Technol. Lett.*, 3, 227–233, doi:10.1021/acs.estlett.6b00150, 2016
- Tranvik, L.J., Downing, J.A., Cotner, J.B., Loiselle, S.A., Striegl, R.G., Ballatore, T.J., Dillon, P., Finlay, K., Fortino, K., Knoll, L.B., and Kortelainen, P.L.: Lakes and impoundments as regulators of carbon cycling and climate, *Limnol. Oceanogr.*, 54, 2298–2314, 2009
- 630 Tudor, M., Teodorof, L., Burada, A., Tudor, M., Ibram, O., and Despina, C.: Long-term nutrients and heavy metals concentration dynamics in aquatic ecosystems of the Danube Delta, *Sci. Ann. Danube Delta Inst.*, 22, 149–156, 2016
- Wang, D., Chen, Z., Sun, W., Hu, B., and Xu, S.: Methane and nitrous oxide concentration and emission flux of Yangtze Delta plain river net, *Sci. China, Ser. B Chem.*, 52, 652–661, doi:10.1007/s11426-009-0024-0, 2009
- Wanninkhof, R.H.: Relationship between wind speed and gas exchange, *J. Geophys. Res.*, 97, 7373–7382, 1992
- 635 Ward, N.D., Bianchi, T.S., Medeiros, P.M., Seidel, M., Richey, J.E., Keil, R.G., and Sawakuchi, H.O.: Where Carbon Goes When Water Flows: Carbon Cycling across the Aquatic Continuum, *Front. Mar. Sci.*, 4, 1–27, doi:10.3389/fmars.2017.00007, 2017
- Wiesenburg, D.A., and Guinasso Jr, N.L.: Equilibrium solubilities of methane, carbon monoxide, and hydrogen in water and sea water, *Journal of chemical and engineering data*, 24, 356-360, 1979
- 640 Woolway, R.I., and Merchant, C.J.: Worldwide alteration of lake mixing regimes in response to climate change, *Nat. Geosci.*, 12, 271–276, doi:10.1038/s41561-019-0322-x, 2019
- Yvon-Durocher, G., Allen, A.P., Bastviken, D., Conrad, R., Gudas, C., St-Pierre, A., Thanh-Duc, N., and Del Giorgio, P.A.: Methane fluxes show consistent temperature dependence across microbial to ecosystem scales, *Nature*, 507, 488–491. doi:10.1038/nature13164, 2014
- 645 Zhang, C., Cheng, S., Long, L., Xie, H., Mu, X., and Zhang, W.: Diel and seasonal methane flux across water–air interface of a subtropic eutrophic pond, *Toxicol. Environ. Chem.*, 100, 413–424, doi:10.1080/02772248.2018.1499231, 2018
- Zuidgeest, A., Baumgartner, S., and Wehrli, B.: Hysteresis effects in organic matter turnover in a tropical floodplain during a flood cycle, *Biogeochem.*, 131, 49-63, doi:10.1007/s10533-016-0263-z, 2016